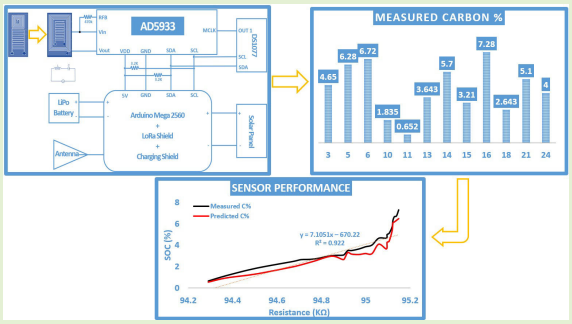
Calibration and Validation of an Embedded AD5933 Impedimetric Sensor System for Soil Organic Carbon Measurement

Waqas A. K. Afridi, *Student Member, IEEE*, Brady Shearan, *Student Member, IEEE*, Bandita Mainali, and Subhas Chandra Mukhopadhyay, *Fellow, IEEE*

***Abstract*—This article presents the development and validation of an embedded sensor system for the measurement of soil organic carbon (SOC) using the AD5933 impedance analyzer integrated with an Arduino microcontroller. The system includes a DS1077 programmable clock and custom shields for real-time field deployment. Calibration was performed using known resistors to derive gain and phase correction parameters essential for accurate resistance-based SOC estimation. Distinct predictive models were formulated for soils with low (⩽4%) and high (⩾4%) carbon concentration to improve precision across various soil types. In low-carbon soils, the system demonstrated strong predictive performance ($R^2 = 0.97$), while the overall model maintained high accuracy ($R^2 = 0.92$) across a 0%–8% SOC range. Compared to a conventional lab-based impedance analyzer (HIOKI IM3536), the proposed system offers comparable accuracy, enhanced portability, and reduced cost. This work highlights the system's potential for precision agriculture through scalable, real-time SOC monitoring.**



***Index Terms*—AD5933, DS1077, impedimetric sensor, Internet of Things (IoT) sensors, precision agriculture, soil organic carbon (SOC).**

I. Introduction

SOIL organi carbon (SOC) is a fundamental component of soil organic matter and a key indicator of soil health, fertility, and sustainability. It plays a central role in the global carbon cycle, influencing carbon exchange between the soil, vegetation, oceans, and atmosphere [1]. The SOC quantity in soil is mainly influenced by the balance between carbon inputs, such as plant residues and root exudates, and outputs like microbial respiration and mineralization [2]. SOC is typically estimated using a conversion factor of 1.72 from soil organic matter, implying that approximately 58% of organic matter is carbon [3], [4]. Among various environmental factors, soil texture, temperature, and moisture are considered the most influential in determining SOC levels [5], [6], [7], [8].

Received 18 February 2026; revised 22 March 2026; accepted 24 March 2026. Date of publication 13 April 2026; date of current version 2 June 2026. The associate editor coordinating the review of this article and approving it for publication was Dr. Nirupama Mandal. *(Corresponding author: Subhas Chandra Mukhopadhyay.)*

The authors are with the School of Engineering, Macquarie University, North Ryde, NSW 2119, Australia (e-mail: waqas.afridi@mq.edu.au; brady.shearan@mq.edu.au; bandita.mainali@mq.edu.au; subhas.mukhopadhyay@mq.edu.au).

Digital Object Identifier 10.1109/JSEN.2026.3680522

While high-resolution laboratory analysis provides precise SOC quantification, it remains costly, labor-intensive, and impractical for large-scale or real-time applications. Proximal sensing technologies, such as visible and near-infrared/short-wave infrared (VNIR/SWIR) spectroscopy, have emerged as alternatives offering faster and nondestructive SOC estimation [9]. However, these approaches often demand complex calibration procedures, are sensitive to external conditions, and are relatively expensive for widespread field deployment [10], [11]. Recent developments in electrochemical and impedance-based sensing show promise but still face challenges with robustness, integration, and adaptability in field environments [12], [13]. To address these gaps, this article presents a novel impedimetric sensing system built on a planar interdigital spiral electrode configuration. The sensor integrates an AD5933 impedance analyzer and DS1077 programmable clock into an Arduino-based embedded system, offering a compact, low-power, and real-time SOC estimation solution [14]. Unlike traditional systems, our approach partitions calibration models for high and low-carbon soils, improving localized accuracy (R^2 up to 0.97) while ensuring affordability and portability. This work details the sensor design, calibration strategy, and performance evaluation using

1558-1748 © 2026 IEEE. All rights reserved, including rights for text and data mining, and training of artificial intelligence and similar technologies. Personal use is permitted, but republication/redistribution requires IEEE permission.
See https://www.ieee.org/publications/rights/index.html for more information.
Authorized licensed use limited to: Gaziantep Islam Bilim ve Teknoloji University. Downloaded on August 08,2026 at 08:18:55 UTC from IEEE Xplore. Restrictions apply.

prepared soil samples, highlighting its suitability for in situ SOC monitoring in precision agriculture and environmental applications.

A. Sensor Design and Fabrication

We have developed two distinct designs for impedimetric sensors, both of which are created on a printed circuit board (PCB). These designs utilize a series configuration of inductance and capacitance and feature interdigital plates as well as spiral coil designs. Each design incorporates capacitive plates to generate electric fields and inductive coils that produce a magnetic field when an alternating current (AC) voltage is applied to the terminals. In both designs, the capacitive and inductive components are connected in series. Those planar impedimetric sensors were designed using Altium Designer 6 and later fabricated using standard PCB manufacturing methods. These include photoresist coating, UV exposure using a mask of the designed layout, chemical etching to define copper traces, and finishing processes such as solder masking. This method ensures precise electrode geometries and signal reliability for impedance-based soil measurements, in line with studies that fabricated integrated development environment (IDE) sensors for chemical and environmental sensing [15], [16]. It is assumed that the soil organic matter exhibits both capacitive and magnetic characteristics. Therefore, the proposed impedimetric sensors can measure SOC with better precision. Section I-B further discusses the design principle of the proposed sensors. Fig. 1(a) displays the initial design of an impedimetric sensor for SOC measurement. In this design, the sections of soil samples that come into contact with the interdigitated electrodes interact with the electric field independently, while the portions exposed to the inductive coils interact with the magnetic field separately. As a result, the sensor may not be able to quantify the overall combined effects of the electric and magnetic fields across the entire soil sample [17]. On the other hand, Fig. 1(b) illustrates a modified version of the planar impedimetric sensor designed for more accurate carbon measurements. This design enables soil samples to interact simultaneously with both electric and magnetic fields, allowing the sensor to measure organic carbon with greater precision. However, effective interaction with organic matter only occurs when the gap between the sensor and the soil sample is reduced to zero. To safeguard against moisture, the sensor is coated with an anti-corrosive epoxy. Additionally, the meander and interdigital coils are connected in series. When an AC voltage is applied across the terminals, the meander coil generates a magnetic field, while the interdigital coil produces an electric field. This combination creates an electromagnetic field that interacts with the test material [18], [19].

B. Inductance–Capacitance Design Principle

The impedimetric sensor has been designed with a combination of inductance and capacitance using an interdigital and spiral structure, which is fabricated to test the dielectric permittivity and magnetic permeability of various soil profiles against the change in organic carbon. To determine the sensitivity of the carbon sensor, the total impedance (Z), assuming

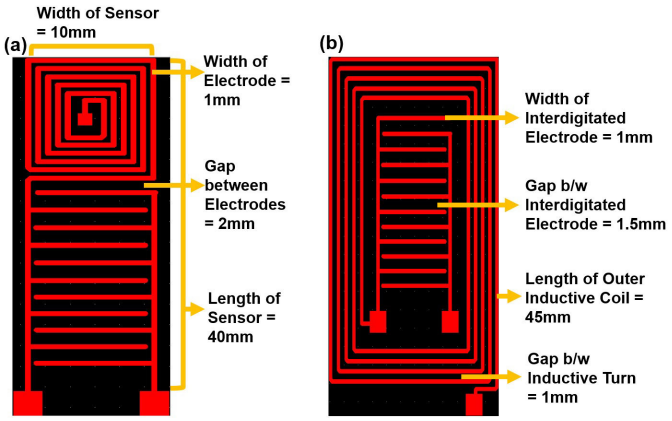


Fig. 1. Design of interdigital impedimetric sensors for SOC measurement. (a) Sensor design 1. (b) Sensor design 2.

no resistance in series, is calculated using the combination of inductor (L) and capacitor (C), as depicted in the following equation:

$$Z = j\omega_L - \frac{j}{\omega_C} \tag{1}$$

where j is the imaginary unit, angular frequency $\omega = 2\pi$f, inductive reactance $\omega_L = 2\pi fL$, and capacitive reactance $\omega_C = 1/2\pi fC$. Thus,

$$Z = j\left(2\pi fL - \frac{1}{2\pi fC}\right). \tag{2}$$

For AC, the magnitude of impedance is

$$|Z| = \left|2\pi fL - \frac{1}{2\pi fC}\right|. \tag{3}$$

This is the absolute value of the net reactance, because inductive and capacitive reactance subtract in series. While (f) represents frequency, (L) denotes inductance, and (C) signifies capacitance. Notably, as the percentage of organic carbon in soil increases, the inductance of the sensor also increases, while its capacitance decreases. Inductance is crucial for calculating changes in impedance, as outlined in (3). However, the total impedance of the sensor system is significantly influenced by frequency. By choosing an appropriate frequency, the system can optimize its sensitivity to variations in soil properties, such as organic carbon content, which in turn affects inductance (L) and capacitance (C).

C. Soil Sample Collection and Preparation

To evaluate the performance of the fabricated sensors for measuring SOC, 25 soil samples were collected from different pastoral areas around New South Wales, Australia. While a sensor node was deployed in a pilot farm located near the Narrabri Airport Weather Station (30°16'05.2"S 149°51'17.6"E) for real-time data collection [20]. The collected samples were then prepared in the laboratory according to standard procedures, which involved drying, grinding, and sieving. All experiments were conducted in a controlled laboratory environment, maintaining a constant temperature of 25 °C and a relative humidity of 40%. Initially, the samples were dried in an oven at 90 °C for 24 h. After drying,

Authorized licensed use limited to: Gaziantep Islam Bilim ve Teknoloji University. Downloaded on August 08,2026 at 08:18:55 UTC from IEEE Xplore. Restrictions apply.

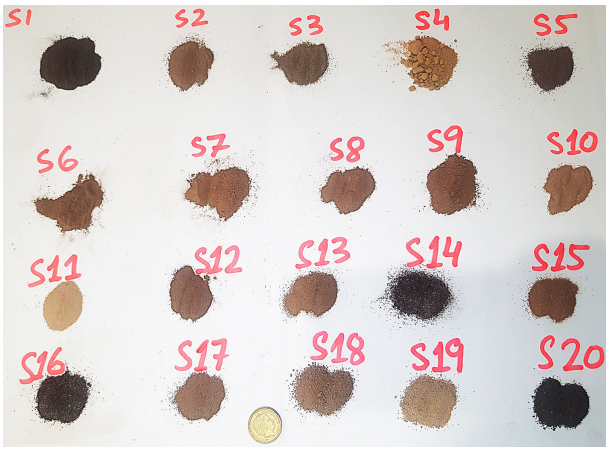


Fig. 2. Prepared soil samples for laboratory testing. Note: 20 out of 25 soil samples are shown; all 25 were used in the sensor testing and data analysis.

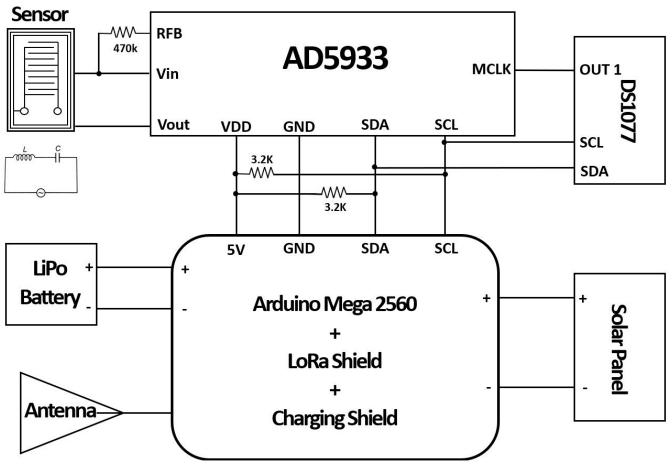


Fig. 3. Connection schematic of the AD5933 sensing system.

the samples were ground and sieved to a size of 2.0 mm or smaller to remove larger organic debris and stored in small, air-tight containers. Fig. 2 illustrates some portion of the samples after preparation. The analysis was conducted using the Walkley–Black (WB) chromic acid wet oxidation method to measure the SOC content in the samples. [12].

II. Sensor Integration Using AD5933 Impedance Analyzer

The integration of the impedimetric sensor with an embedded AD5933 impedance analyzer setup represents a critical step in transitioning soil carbon measurement from controlled laboratory settings to practical field deployment [21]. By interfacing the sensor with an Arduino Mega 2560 microcontroller through a dedicated AD5933 impedance analyzer shield, the system is transformed into a compact, low-power, and portable solution capable of continuous impedance measurement. AD5933 IC was chosen for its affordable integrated impedance measurement features, which include an onboard frequency generator for rapid frequency sweeping and a 12-bit ADC, making it suitable for compact, low-power sensor applications [22], [23]. While Arduino Mega 2560 was chosen due to its high number of I/O pins, multiple serial communication ports, and ample memory, which were needed to handle multiple peripherals, including the sensor, AD5933 impedance measurement IC, external DS1077 clock, and LoRa communication shield. Its compatibility with open-source libraries and ease of hardware interfacing made it suitable for rapid prototyping of embedded sensing systems [24]. This hardware–software integration allows for rapid analysis, reducing the need for time-consuming and resource-intensive laboratory-based methods such as chemical titration or dry combustion techniques [11]. A key aspect of the AD5933 impedance measurement setup involved calibrating the feedback resistor to obtain unity gain and phase correction parameters across a characterization frequency range [25]. These calibration steps are essential for compensating signal distortion and improving the precision of organic carbon measurements [26]. Furthermore, a calibration code was customized and uploaded to the Arduino microcontroller to automate measurement cycles at frequency sweeps and communicate through a long-range wide area network (LoRaWAN) shield [27]. The result is a portable sensing system that balances accuracy and operational simplicity, marking a significant advancement toward decentralized, sensor-driven soil quality monitoring [5].

A. System Design Architecture

The connection schematic in Fig. 3 illustrates the integration of an impedimetric sensor with an Arduino Mega 2560 microcontroller through an AD5933 impedance analyzer IC. The system includes a programmable clock DS1077 for frequency control, a microcontroller for data processing, a LoRa shield for wireless data transmission to a cloud ThingSpeak server, as well as a solar panel and a charging shield for battery charging [28]. Moreover, a feedback resistor of 470 kΩ is used with the AD5933 impedance analyzer to enhance the sensor sensitivity against low-conductivity soil. The communication between devices within the system is done via I^2C protocol using serial data (SDA) and serial clock (SCL) signals. The DS1077 programmable oscillator provides the necessary clock signal to the AD5933. Power is supplied through a combination of a lithium-polymer battery and a 6-V, 6-W solar panel, ensuring autonomous operation in remote locations [29]. This setup can determine carbon percentage in the soil using impedance measurement from Arduino IDE, serving as an alternative to traditional laboratory testing methods. To support reproducibility, the model and version of key components and software used in the study are listed in Table I.

B. AD5933 Impedance Analyzer

The high-precision AD5933 impedance analyzer IC calculates both the real and imaginary components of impedance at selected frequencies using discrete Fourier transforms (DFTs). This IC is designed for electrochemical impedance spectroscopy (EIS) analysis and offers exceptional accuracy. However, before taking sensor measurements, it is essential to calibrate both the feedback resistor and the system's gain factor and phase values to ensure precise analysis. It is crucial

Authorized licensed use limited to: Gaziantep Islam Bilim ve Teknoloji University. Downloaded on August 08,2026 at 08:18:55 UTC from IEEE Xplore. Restrictions apply.

TABLE I
COMPONENTS AND SOFTWARE USED IN THE PROPOSED SYSTEM

Component / Software	Model / Version	Manufacturer
Arduino Mega 2560	Rev3	Arduino LLC
Impedance Analyzer IC	AD5933	Analog Devices Inc.
Programmable Clock	DS1077Z	Maxim Integrated
LoRa Shield	SX1276, 915MHz	Semtech Corporation
Solar Charger Shield	v2.2	Seeed Studio
Solar Panel	6V, 6W Monocrystaline	Adafruit
Lithium-Polymer Battery	3.7V, 6000mAh	Generic/Commercial
Dipole Antenna	3dBi, 900MHz	Generic/LoRa compatible
LoRa Gateway	OLG01	Dragino Technology Co.
Sensor PCB Material	FR-4	Generic PCB Fabricator
LCR Meter	IM3536	HIOKI E.E. Corporation
Arduino IDE	Version 1.8.19	Arduino LLC
MATLAB	Version R2022a	MathWorks Inc.
Altium Designer	Version 6	Altium Limited

TABLE II
CLOCK FREQUENCY REQUIREMENTS FOR AD5933 OPERATION

AD5933 Lower Frequency	Clock Frequency Applied to MCLK Pin
100 kHz to 5 kHz	16 MHz
5 kHz to 1 kHz	4 MHz
5 kHz to 300 Hz	2 MHz
300 Hz to 200 Hz	1 MHz
200 Hz to 100 Hz	250 kHz
100 Hz to 30 Hz	100 kHz
30 Hz to 20 Hz	50 kHz
20 Hz to 10 Hz	25 kHz

to choose a resistor value that maintains unity gain, as any variations in this gain can lead to instability in the operational amplifier. The unity gain is sustained through the following equation:

$$\frac{R_F}{R_{in}} = 1. \tag{4}$$

C. DS1077 Programmable Clock

The DS1077Z is a programmable solid-state oscillator that generates frequencies from 12.2 kHz to 100 MHz. Integrated into the system, it provides an adjustable clock signal for the AD5933, enabling impedance analysis below 3 kHz. The AD5933 typically uses a 16.776-MHz internal oscillator for frequencies between 3 and 100 kHz, but with an external clock input, it can analyze from 10 Hz to 3 kHz. This clock is programmable via I^2C, using a provided example program. The manufacturer has supplied a table of external clock frequencies needed for analysis, as shown in Table II.

The characterization frequency range for our carbon sensor is 175–225 Hz using a 1-MHz clock input as shown in 5. The application of low-frequency measurements is supported by a study that employed four-electrode low-frequency impedance measurements utilizing the AD5933 chip. This approach underscores the efficacy of low-frequency techniques in impedance analysis, highlighting their relevance in various research contexts [30], [31]. The system operates by adjusting the primary clock frequency of 16.776 MHz, which can be scaled down by factors of 1, 2, 4, or 8 using the pre-scaler block P1. Additionally, the divider block "N" can further reduce the frequency by factors of 2, up to a maximum of 1024. Thus, to produce a 1-MHz frequency, the P1 block is set to 8 and the N block to 2

$$Freq = \frac{Primary}{P1 * N} = \frac{16.776\,MHz}{(8) * (2)} = 1.045\,MHz. \tag{5}$$

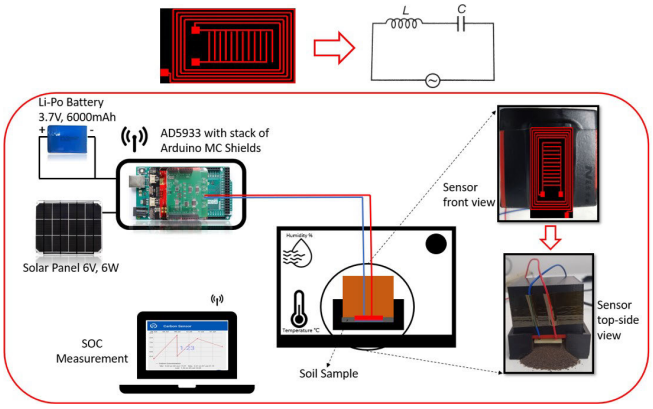


Fig. 4. Experimental setup for AD5933 calibration and sensor testing.

To achieve the desired results, the programmable registers must be correctly configured. This includes setting the mode of operation for the Multiplexer (MUX), the operating frequency for division multiplexing (DIV), and the bus settings (BUS). For this application, to set P1 to 8, both the "1M1" and "1M0" MUX bits should be set to 1, while the DIV1 bit needs to be set to 0 to establish "N" as 2.

D. Experimentation and Calibration Method of AD5933

The schematic for the experimental setup used in the calibration and testing of the AD5933 sensor is shown in Fig. 4. As illustrated, the sensor is mounted on a 150-g 3-D-printed square weight designed to ensure that it maintains good contact with the soil sample. This setup allows for optimal interaction with various soil textures within the 3-D container. Additionally, a stack of Arduino shields is connected to the sensor for impedance measurements. In this study, resistance (R) is preferred over full impedance for calibrating the AD5933 sensor because it exhibits a stronger and more consistent correlation with SOC. Resistance, as the real component of impedance, effectively captures the conductive behavior of the soil matrix, which is influenced by moisture, ionic concentration, and organic matter. This simplification enhances model development and improves accuracy [32]. In contrast, impedance (Z) tends to show higher variability and less intuitive scaling due to capacitive and inductive elements. These elements are more sensitive to environmental changes, frequency, and sensor alignment, making calibration more complex and reducing efficiency. This choice facilitates real-time, scalable deployment in the field, which is essential for precision agriculture [33]. Furthermore, the calibration of the AD5933 needs adjustments to both the feedback resistor and the system gain factor along with the phase values before conducting sensor measurements. To achieve this, we must first identify the operating frequency and resistance range of the sensor during the characterization step [34]. Moreover, it is essential to experiment with various known resistances through trial and error while calibrating AD5933 across the anticipated range of measurable resistances. In our case, the sensor characterization frequency range is between 175 and 225 Hz, and the resistance maintained in that range is from 100 to 500 kΩ. By performing calibration trials and verifying the accuracy of each feedback resistor (RFB), we tested a variety of known

Authorized licensed use limited to: Gaziantep Islam Bilim ve Teknoloji University. Downloaded on August 08,2026 at 08:18:55 UTC from IEEE Xplore. Restrictions apply.

resistances to minimize the error between the implemented feedback resistor and the value measured by the AD5933 system on the IDE serial monitor. Ultimately, the feedback resistor used in the final system is 470 kΩ. The feedback resistor implemented in the system enabled the AD5933 to maintain a measurement difference of less than 0.5% and is prepared to be used alongside the sensor. AD5933 is equipped with a pre-coded Arduino library [35], which simplifies the calibration process for both the gain factor and phase while also saving these values for future reference. Calibration is achieved using R_{CAL} across a broad frequency sweep

$$\mathrm{R_{CAL}} = (\mathrm{Z_{MIN}} + \mathrm{Z_{MAX}}) \times \frac{1}{3}. \tag{6}$$

The phase calculation is relative, where the phase of the unknown impedance is derived from the phase of the initially calibrated system. The system phase is first determined in conjunction with R_{CAL}

$$\varnothing_{ph} = \tan^{-1}\left(\frac{Z_{IMAG}}{Z_{REAL}}\right). \tag{7}$$

Then, the calibration resistor is replaced with a known resistance, allowing the measured phase to be determined using

$$\varnothing_{ph} = (\varnothing_{UNKNOWN} - \varnothing_{SYSTEM}). \tag{8}$$

The system accuracy was evaluated using various known resistances and validated with laboratory equipment. It demonstrated a measurement difference of less than 0.5%, indicating that it is ready for use with the sensor.

III. Results: Sensor Performance Evaluation

Fig. 5 illustrates the sensor performance results for organic carbon measurement and prediction across the total collected soil samples, using resistance data acquired from an AD5933 impedance analyzer shield. The predictive model (red) closely follows the measured data (blue), particularly across the mid-range of carbon percentages, while some underestimation is observed at the upper extreme. Despite minor fluctuations, the model achieves a high R^2 value of 0.9224, indicating strong agreement and reliability. The fit equation $y = 7.1051x - 670.22$ reflects a generally consistent relationship between resistance and organic carbon across a broader range. Nonetheless, this performance discrepancy indicates the model's sensitivity limit in the sensor's nonlinear impedance range. To address the limitation and enhance precision across the full SOC spectrum, the data were split into two distinct regimes, resulting in the development of two separate fitting models optimized for low and high carbon concentrations. This adaptive modeling approach is in line with a study that proposed two calibration models for SOC estimation by transforming 1-D data into 2-D spectrograms, allowing for rapid in-field estimation of SOC while maintaining accuracy across different soil types and organic matter levels [36].

Fig. 6 illustrates the performance of the AD5933 sensor setup in estimating organic carbon in soils with carbon levels below 4%. The low-carbon model demonstrates a high predictive accuracy. The close alignment between the measured

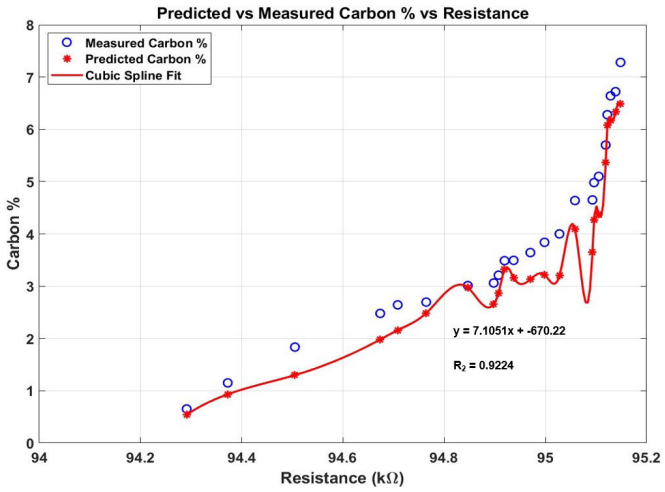


Fig. 5. Predictive model for SOC across all samples using Sensor-AD5933 setup.

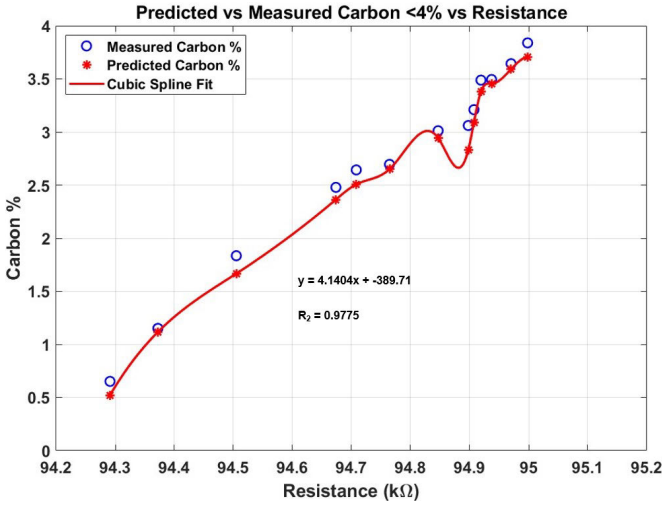


Fig. 6. Predictive model for SOC below 4% using Sensor-AD5933 setup.

(blue) and predicted (red) carbon across the resistance range of 94–96 kΩ. The minimal deviation between the two curves indicates consistent performance with the model effectively capturing the trend of increasing carbon with increasing resistance. The fit linear equation $y = 4.1404x - 389.71$ and the R^2 value of 0.97 confirm a strong correlation and excellent goodness of fit, making the model highly reliable for low-carbon soil conditions [37].

Fig. 7 illustrates the prediction model designed explicitly for soils with organic carbon exceeding 4%. This separate model shows good predictive accuracy for higher carbon concentrations, particularly in the range of 4%–8%. Although there are slight underestimations at certain points around 4%–4.5%, the predicted carbon (red) remains closely aligned with the measured values (blue) across the entire resistance range. The linear model expressed as $y = 28.1520x - 2672.10$ demonstrates a steeper slope, which accurately captures the sharper increase in organic carbon at higher resistance, particularly beyond 95 kΩ. The R^2 value of 0.8810 indicates a good correlation and fitness of the model. Although it is not as

Authorized licensed use limited to: Gaziantep Islam Bilim ve Teknoloji University. Downloaded on August 08,2026 at 08:18:55 UTC from IEEE Xplore. Restrictions apply.

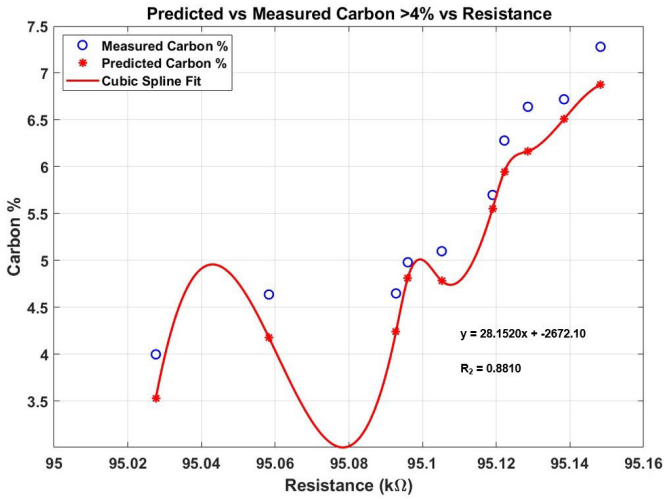


Fig. 7. Predictive model for SOC above 4% using Sensor-AD5933 setup.

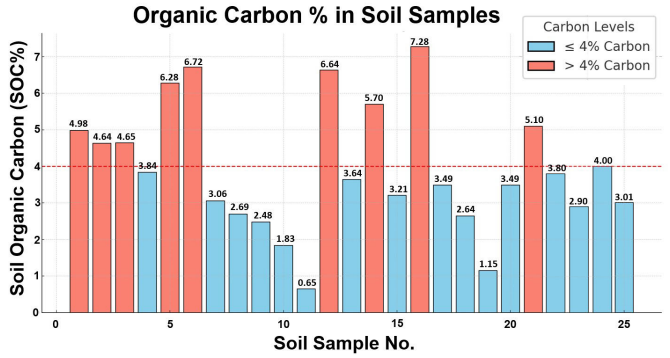


Fig. 8. Grouping of measured organic carbon across all prepared soil samples.

accurate as the model for soils under 4% carbon, it improved the reliability of predictions for higher carbon soils, validated the approach of segmenting data range to enhance model precision [36].

A. Organic Carbon Grouping Across All Soil Samples

The bar chart in Fig. 8 illustrates the distribution of SOC percentages across 25 prepared soil samples. The measured samples are segmented into two groups of low and high organic carbon concentrations to maintain precision across different soil types and organic matter levels. The sensor's ability to distinctly capture this variance across a broad range from as low as 0.65% to as high as 7.28% demonstrates its robust sensitivity and accuracy across diverse soil types. The close clustering of values around the threshold line (4%) and the clear delineation between low and high carbon soils validate the sensor's impedance-based calibration model and its effectiveness in differentiating subtle compositional changes. Notably, consistency is observed in both high-carbon and low-carbon soil groups without abnormal fluctuations or false groupings, which affirms the reliability of the developed carbon sensor even under variable soil textures and moisture conditions. From an agronomic perspective, it is important to closely assess SOC levels to shape precision farming strategies. High SOC levels usually mean better soil health, which includes greater fertility, improved water retention, and more active microorganisms. These factors are crucial for healthy soil. Conversely, soils with low organic carbon identified through the proposed sensor can be targeted for soil amendments or organic matter enrichment. Hence, the sensor's real-time functionality, affordability, and compatibility with smart farming systems make it an ideal tool for scalable and site-specific soil management.

IV. Error Analysis

The error evaluation metrics in Table III provide a comprehensive assessment of the model's reliability across all soil samples, using the calibrated AD5933 impedance analyzer-sensor setup. The mean absolute error (MAE) of 0.45 and the root-mean-square error (RMSE) of 0.11 indicate that the model can perform with high accuracy, particularly in field applications where minor deviations in carbon estimation are generally acceptable. The MAE suggests that, on average, the predicted SOC percentage deviates by less than half a percent from the actual measured values, which is an impressive result considering the complexity of soil composition and field conditions. While examining the samples individually, the absolute errors range from 0.04 to 0.99, indicating variability based on carbon concentration. Lower errors are observed in the middle range of carbon concentration, specifically in Samples 6–11 and 20–24. Some samples showed moderate prediction errors, while higher errors appeared in more carbon-concentrated samples 13 to 19 and 25, which is in line with the study that attributed significant errors in higher SOC concentrated samples due to inconsistent sample processing [38]. This suggests that the model may underperform at the head of the dataset, likely due to the nonlinear relationship between resistance and SOC concentration not being fully captured by a single exponential model. Thus, there was a need to develop separate models for low- and high-carbon samples, which could enhance localized accuracy. Despite these outliers, the overall model for the complete measurement range demonstrates good consistency and applicability, as indicated by an R-squared value of 0.9217 and an adjusted R-squared value of 0.918. These metrics show that over 92% of the variance in measured SOC can be explained by the overall predictive model.

A. Visualizing Prediction Error Across All Samples

The error bar plot in Fig. 9 provides a visual assessment of prediction error across the full resistance range for overall measured SOC. Each red data point represents a measured SOC value, while the black vertical bars indicate the absolute prediction error for each sample. The mean error shown as a dashed blue line at 0.454, along with the maximum error of 0.99, offers key reference points for evaluating model performance. Notably, the error magnitude increases slightly at higher resistance values, particularly beyond 95.1 kΩ, suggesting a higher variability in prediction accuracy for soils with greater carbon concentration. Despite this, most errors remain within an acceptable range, reinforcing the model's

Authorized licensed use limited to: Gaziantep Islam Bilim ve Teknoloji University. Downloaded on August 08,2026 at 08:18:55 UTC from IEEE Xplore. Restrictions apply.

TABLE III
SOC ESTIMATION USING RESISTANCE AND MODEL ERROR ANALYSIS

Soil Sample	Resistance (k)	Measured Carbon (%)	Predicted Carbon (%)	Absolute Error
1	94.29097	0.652	0.761	0.109
2	94.37209	1.151	0.932	0.219
3	94.50489	1.835	1.299	0.536
4	94.6735	2.479	1.980	0.499
5	94.7082	2.643	2.159	0.484
6	94.76428	2.695	2.485	0.210
7	94.8466	3.012	3.052	0.040
8	94.89773	3.061	2.654	0.407
9	94.90722	3.21	3.552	0.342
10	94.91906	3.488	3.658	0.170
11	94.93705	3.494	3.827	0.333
12	94.97009	3.643	4.156	0.513
13	94.99809	3.839	4.458	0.619
14	95.0276	4.000	4.799	0.799
15	95.05826	4.638	5.181	0.543
16	95.092831	4.65	5.649	0.999
17	95.09599	4.982	5.694	0.712
18	95.10347	5.12	5.801	0.681
19	95.10518	5.10	5.826	0.726
20	95.11036	5.42	5.902	0.482
21	95.11896	5.70	6.030	0.330
22	95.12216	6.28	6.079	0.201
23	95.12859	6.64	6.177	0.463
24	95.13842	6.72	6.331	0.389
25	95.14828	7.28	6.489	0.791

Model Summary (General model Exp1)
$f(x) = a \cdot \exp(bx)$
Coefficients (with 95% confidence bounds):
$a = 3.208 \times 10^{-103}$ $(-1.346 \times 10^{-101}, 1.41 \times 10^{-101})$
$b = 2.5$ $(2.048, 2.951)$
Goodness of Fit:
SSE = 5.418
MAE = 0.45
$R^2 = 0.9217$
Adjusted $R^2 = 0.918$
RMSE = 0.11

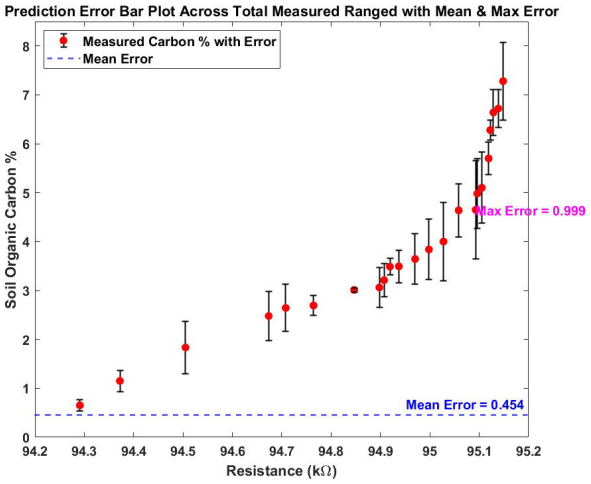


Fig. 9. Error bar plot of SOC % prediction with mean and maximum error.

overall consistency and reliability. The concentration of shorter error bars in the mid-resistance region further supports the sensor's strong performance in the moderate-carbon range with room for refinement at the extremes.

B. Visualizing Prediction Error in Samples Under 4% Carbon

The error bar plot in Fig. 10 for SOC prediction in soils under 4% measured carbon illustrates the model's strong predictive accuracy and consistency. The red data points are the measured values, while the black error bars indicate prediction deviations. Most error bars are tightly clustered confirming low variability and high repeatability. The mean error marked as a dashed blue line at 0.345 is well within acceptable limits for field measurements and the maximum

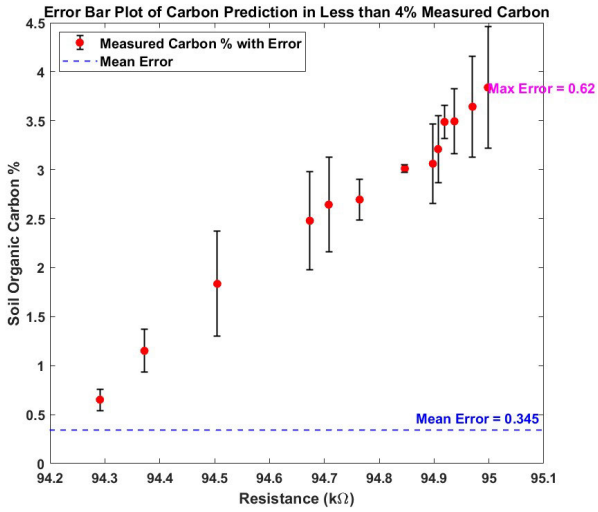


Fig. 10. Error bar plot of SOC prediction in less than 4% measured carbon.

error of 0.62 occurs only once, indicating rare outlier behavior. These results underscore the reliability of the low-carbon model, making it particularly effective for characterizing soils with minimal organic carbon. The consistent performance across the resistance range further validates the system's practical suitability for precision agriculture and environmental monitoring in carbon-depleted soils.

C. Visualizing Prediction Error in Samples Over 4% Carbon

The error bar plot in Fig. 11 for samples with over 4% carbon reveals a modest increase in prediction variability compared to lower carbon samples. The red data points and associated error bars highlight that while most predictions remain reasonably close to actual values, the spread is wider in the upper range. The mean error is slightly elevated at 0.595, and the maximum error peaks at 0.999, indicating a few samples where the model underperforms. The longer error bars around resistance values from 95.08 to 95.11 kΩ suggest increased uncertainty at higher SOC levels, likely due to the nonlinear relationship between impedance and organic carbon becoming harder to generalize. Despite this, the model still maintains usability for higher carbon soils offering quick, field-deployable estimates. However, further refinement or additional calibration in this range could enhance accuracy and robustness.

D. Improvements in Accuracy, Repeatability, Sensitivity, and Portability

The calibrated AD5933-based system marks a significant improvement over conventional lab-based impedance analyzers, such as the HIOKI IM3536, in several key areas. Despite the AD5933 being a compact and low-power IC, the system achieves comparable measurement accuracy within its calibrated range, validated by a high R^2 value of 0.9217 and an adjusted R^2 of 0.918. Particularly when carbon concentration is below 4%, the system exhibited high predictive accuracy with minimal absolute errors, confirming its effectiveness in

Authorized licensed use limited to: Gaziantep Islam Bilim ve Teknoloji University. Downloaded on August 08,2026 at 08:18:55 UTC from IEEE Xplore. Restrictions apply.

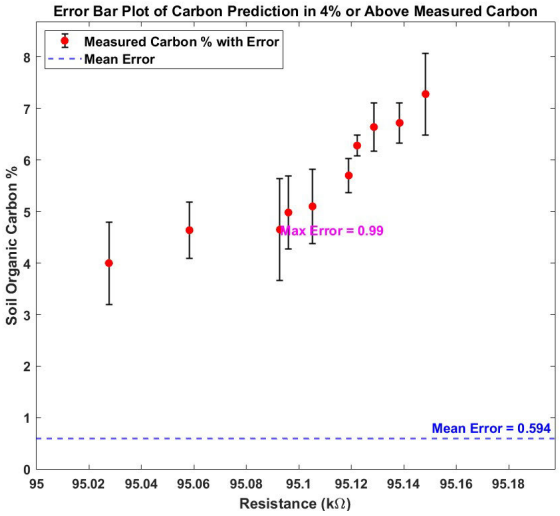


Fig. 11. Error bar plot of SOC prediction in 4% or above measured carbon.

identifying early stage or low-carbon soils. However, as the carbon concentration increases and approaches a maximum of 8%, the model's accuracy starts to decline, as indicated by rising absolute errors for those samples. This performance divergence reflects the model's sensitivity limit within the nonlinear range of the sensor's impedance response. Its performance is further enhanced by repeatable frequency sweep measurements, as indicated by the narrow error range and low SSE (5.418). In terms of sensitivity, the sensor effectively distinguishes even subtle changes in electrical resistance as the real component of impedance translated into SOC within its calibrated range relevant to soil health diagnostics. From a practical standpoint, the proposed AD5933-based system's portability, low cost, and power efficiency make it suitable for in situ field measurements, eliminating the need to transport samples to a laboratory. This approach not only reduces time and labor but also enables more frequent and spatially distributed monitoring [11], [23], [26], [39]. It can be easily scaled across different soil types, which is essential for precision agriculture and environmental assessment.

E. Discussion of Limitations

While the proposed embedded impedimetric sensor system offers a scalable and low-cost solution for SOC estimation, several limitations affect its broader deployment and long-term reliability. First, maintaining signal integrity during impedance measurements remains a challenge, particularly in heterogeneous soil environments where moisture, temperature, and ionic content can introduce variability. Although the DS1077 external clock enhanced frequency precision for the AD5933 impedance analyzer, it also introduced greater susceptibility to electrical noise, necessitating high-quality PCB layout and shielding practices. Another key limitation lies in the calibration process. The system's performance relies on stable resistance-based measurements, and gain and phase calibration of the AD5933 was done manually using known resistors. However, this calibration can drift over time due to environmental changes, requiring periodic recalibration to retain accuracy. Power management also presented a constraint, especially when combining solar charging, LiPo batteries, and LoRa transmission for real-time monitoring. Achieving efficient energy consumption demanded synchronized sleep-wake cycles, which can be difficult to maintain under field conditions. Finally, physical deployment issues such as soil contact inconsistencies and the need for effective waterproofing and tillage resistance pose risks to sensor durability and data accuracy. Despite these limitations, the system demonstrates promise, but future iterations should consider robust enclosure design, automated recalibration routines, and improved noise isolation to enhance operational resilience and scalability.

V. Conclusion and Future Work

The study contributes to the design and integration of a novel impedimetric sensor with an embedded microcontroller system for measuring SOC. By utilizing interdigital and spiral inductive–capacitive geometries on FR-4 PCBs and integrating these with the AD5933 impedance analyzer and DS1077 clock, we developed a robust sensor platform. This system was calibrated against the WB chemical titration method and validated through over 1000 test runs. It achieved an overall R^2 value of 0.92, an MAE of 0.45, and an RMSE of 0.11, demonstrating strong performance in both low and high carbon soils. The strength of this solution lies in its seamless integration of low-cost hardware with advanced analytics, effectively addressing both scalability and accuracy in agricultural settings. The proposed system has significant potential for commercial rollout, especially in developing countries where budget constraints limit access to proprietary environmental monitoring tools. While the current system overcomes key limitations of traditional monitoring methods, there are several opportunities to further expand, refine, and scale this work. Future iterations of the proposed system could utilize more compact microcontrollers like ESP32 or low-power STM32 series to enable on-node edge computing, thereby reducing data transmission needs. Updating the PCB design to include built-in analog-to-digital converters (ADCs) and multiplexers can help reduce noise and improve analog signal quality. The sensor system is designed for shallow deployment (5–10 cm depth) for on-site SOC measurements, suitable for temporary use in soil and compatible with handheld or drone-mounted operations. Future developments may include protective housing against farm machinery for semi-permanent deployments. Implementing automatic calibration routines with memory logging during power loss can also improve the system's reliability [40]. Furthermore, adaptive filtering techniques, such as the Kalman filter or Savitzky–Golay filter, can improve signal stability of the sensor under varying field conditions [41], [42].

References

[1] D. Crisp et al., "How well do we understand the land-ocean-atmosphere carbon cycle?" *Rev. Geophys.*, vol. 60, no. 2, pp. 1–64, 2022.

[2] T. Saarela et al., "Dissolved organic matter composition regulates microbial degradation and carbon dioxide production in pristine subarctic rivers," *Biogeosciences Discuss.*, pp. 1–28, Nov. 2022.

[3] J. E. Ayala Izurieta et al., "Improving the remote estimation of soil organic carbon in complex ecosystems with sentinel-2 and GIS using Gaussian processes regression," *Plant Soil*, vol. 479, nos. 1–2, pp. 159–183, Oct. 2022.

[4] A. C. Abdullahi, C. Siwar, M. I. Shaharudin, and A. Isahak, "Carbon sequestration in soils: The opportunities and challenges," *Carbon Capture*, pp. 3–16, Sep. 2018.

Authorized licensed use limited to: Gaziantep Islam Bilim ve Teknoloji University. Downloaded on August 08,2026 at 08:18:55 UTC from IEEE Xplore. Restrictions apply.

[5] W. A. Afridi, F. Akhter, I. Vitoria, and S. C. Mukhopadhyay, *A Technology Review and Field Testing of a Soil Water Quality Monitoring System*, vol. 1035. Cham, Switzerland: Springer Nature, 2023.

[6] E. Hobley, B. Wilson, A. Wilkie, J. Gray, and T. Koen, "Drivers of soil organic carbon storage and vertical distribution in eastern Australia," *Plant Soil*, vol. 390, nos. 1–2, pp. 111–127, May 2015.

[7] R. Baumhardt, B. Stewart, and U. Sainju, "North American soil degradation: Processes, practices, and mitigating strategies," *Sustainability*, vol. 7, no. 3, pp. 2936–2960, Mar. 2015.

[8] V. S. Patil, S. A. Shinde, and N. M. Dhawale, "A review on determination of soil organic matter and soil moisture content using conventional methods and image processing techniques," in *Proc. IEEE Pune Sect. Int. Conf. (PuneCon)*, Dec. 2021, pp. 1–6.

[9] N. M. Dhawale, V. I. Adamchuk, S. O. Prasher, and R. A. V. Rossel, "Evaluating the precision and accuracy of proximal soil vis–NIR sensors for estimating soil organic matter and texture," *Soil Syst.*, vol. 5, no. 48, pp. 1–19, 2021.

[10] V. N. Dhamu, A. C. Somenahally, A. Paul, S. Muthukumar, and S. Prasad, "Characterization of an in-situ soil organic carbon (SOC) via a smart-electrochemical sensing approach," *Sensors*, vol. 24, no. 1153, pp. 1–13, Feb. 2024.

[11] N. Loria, R. Lal, and R. Chandra, "Handheld in situ methods for soil organic carbon assessment," *Sustainability*, vol. 16, no. 13, Jun. 2024, Art. no. 5592.

[12] F. Akhter, K. P. Jayasundera, A. K. A. S, B. Shearan, and W. A. Afridi, *Initial Studies for a Novel Electromagnetic Sensor for Detection of Carbon Content in Soil*, vol. 1. Sydney, NSW, Australia: Springer Nature, 2023.

[13] W. A. K. Afridi, S. C. Mukhopadhyay, and B. Mainali, "Machine learning enabled smart sensor node for evapotranspiration prediction in diverse soil and environmental conditions," *IEEE Sensors J.*, vol. 25, no. 12, pp. 22720–22728, Jun. 2025.

[14] S. J. Juneidi, "Smart greenhouses using Internet of Things: Case study on tomatoes," *Int. J. Smart Sens. Intell. Syst.*, vol. 15, no. 1, pp. 1–15, Jan. 2022.

[15] A. Gupta, P. Dakhare, R. Bhagat, D. Rotake, and A. D. Darji, "Fabrication of printed circuit board interdigitated electrode sensor for cadmium detection," in *Proc. IEEE 8th Int. Conf. Converg. Technol. (I2CT)*, Apr. 2023, pp. 1–6.

[16] F. Perdigones and J. Quero, "Printed circuit boards: The Layers' functions for electronic and biomedical engineering," *Micromachines*, vol. 13, no. 3, p. 460, Mar. 2022.

[17] W. A. K. Afridi et al., "Design an electromagnetic sensor to measure the organic carbon in soil and its validation with standard walkley–black method," *IEEE Sensors Lett.*, vol. 7, no. 12, pp. 1–4, Dec. 2023.

[18] S. C. Mukhopadhyay, "A novel planar mesh-type microelectromagnetic sensor. Part II: Estimation of system properties," *IEEE Sensors J.*, vol. 4, no. 3, pp. 308–312, Jun. 2004.

[19] M. A. M. Yunus and S. C. Mukhopadhyay, "Novel planar electromagnetic sensors for detection of nitrates and contamination in natural water sources," *IEEE Sensors J.*, vol. 11, no. 6, pp. 1440–1447, Jun. 2011.

[20] G. Gupta and R. Van Zyl, "Energy harvested end nodes and performance improvement of LoRa networks," *Int. J. Smart Sens. Intell. Syst.*, vol. 14, no. 1, pp. 1–15, Jan. 2021.

[21] W. A. K. Afridi, I. Vitoria, K. Jayasundera, S. C. Mukhopadhyay, and Z. Liu, "Development and field installation of smart sensor nodes for quantification of missing water in soil," *IEEE Sensors J.*, vol. 23, no. 21, pp. 26495–26502, Nov. 2023.

[22] R. Tawie and E. Da'ud, "Low-cost impedance approach using AD5933 for sensing and monitoring applications," in *Proc. Int. Conf. Adv. Manuf. Ind. Appl.*, vol. 429, Seattle, WA, USA, 2018, pp. 1–3.

[23] P. Ibba et al., "Design and validation of a portable AD5933–based impedance analyzer for smart agriculture," *IEEE Access*, vol. 9, pp. 63656–63675, 2021.

[24] A. Shaout, K. Juzswik, K. Nguyen, H. Peurasaari, and A. S. Awad, "An embedded system for agricultural monitoring of remote areas," in *Proc. 11th Int. Comput. Eng. Conf. (ICENCO)*, Dec. 2015, pp. 58–67.

[25] B. Shearan, F. Akhter, and S. C. Mukhopadhyay, "Development of an IoT-enabled portable sulphur sensor: A tutorial paper," *IEEE Sensors J.*, vol. 22, no. 11, pp. 10075–10088, Jun. 2022.

[26] Z. Tan, Q. Feng, T. Ma, J. Zhang, and Y. Liang, "Development of an AD5933-based impedance calibration and measurement technology using piezoceramic transducers," *Measurement*, vol. 210, no. 112527, Mar. 2023, Art. no. 112527.

[27] W. A. K. Afridi, I. Vitoria, and S. C. Mukhopadhyay, "Development of IoT soil sensor node: Installation and modeling," in *IoT Sensors, ML, AI and XAI: Empowering A Smarter World*. Cham, Switzerland: Springer Nature, 2024, pp. 75–90.

[28] A. James, A. Seth, and S. C. Mukhopadhyay, "IoT enabled sensor node: A tutorial paper," *Int. J. Smart Sens. Intell. Syst.*, vol. 13, no. 1, pp. 1–18, Jan. 2020.

[29] W. A. K. Afridi, S. C. Mukhopadhyay, and I. Vitoria, "Multi-depth capacitive soil sensor node testing and deployment," in *Proc. 16th Int. Conf. Sens. Technol. (ICST)*, Dec. 2023, pp. 1–5.

[30] C. Margo, J. Katrib, M. Nadi, and A. Rouane, "A four-electrode low frequency impedance spectroscopy measurement system using the AD5933 measurement chip," *Physiological Meas.*, vol. 34, no. 4, pp. 391–405, Apr. 2013.

[31] A. Piccardi, S. Pettinato, M. C. Rossi, and M. Girolami, "Low-frequency measurements in electrochemical impedance spectroscopy: A brief review," *Electronics*, vol. 14, no. 4048, pp. 1–24, 2025.

[32] A. J. Merritt et al., "Measurement and modelling of moisture—Electrical resistivity relationship of fine-grained unsaturated soils and electrical anisotropy," *J. Appl. Geophysics*, vol. 124, pp. 155–165, Jan. 2016.

[33] I. Ünal, Ö. Kabas, and S. Sözer, "Real-time electrical resistivity measurement and mapping platform of the soils with an autonomous robot for precision farming applications," *Sensors*, vol. 20, no. 251, pp. 1–16, Jan. 2020.

[34] B. K. Cyril and G. Boby, "A capacitive sensing system for non-contact: Detection of ice," *Int. J. Smart Sens. Intell. Syst.*, vol. 7, no. 5, pp. 1–6, Jan. 2014.

[35] *GitHub–A Simple Library for Controlling the AD5933 Impedance Converter System With an Arduino Compatible Device.*, GitHub, Inc., San Francisco, CA, USA, 2015. Accessed: May 19, 2025.

[36] Z. Tong and L. Liu, "SpatialFormer: A model to estimate soil organic carbon content using spectral and spatial information," *J. Soil Sci. Plant Nutrition*, vol. 25, no. 2, pp. 3259–3271, Jun. 2025.

[37] L. Wang, G. Abramowitz, Y.-P. Wang, A. Pitman, and R. A. V. Rossel, "An ensemble estimate of Australian soil organic carbon using machine learning and process-based modelling," *Soil*, vol. 10, no. 2, pp. 619–636, Sep. 2024.

[38] R. J. Even, B. Megan, B. Machmuller, J. M. Lavallee, J. T. Zelikova, and M. F. Cotrufo, "Large errors in common soil carbon measurements due to sample processing," *Soil*, vol. 11, no. 1, pp. 17–34, 2025.

[39] K. Chabowski, T. Piasecki, A. Dzierka, and K. Nitsch, "Simple wide frequency range impedance meter based on AD5933 integrated circuit," *Metrology Meas. Syst.*, vol. 22, no. 1, pp. 13–24, 2015.

[40] S. Mansoor, S. Iqbal, S. M. Popescu, S. L. Kim, Y. S. Chung, and J.-H. Baek, "Integration of smart sensors and IoT in precision agriculture: Trends, challenges and future prospectives," *Frontiers Plant Sci.*, vol. 16, pp. 1–21, May 2025.

[41] Sivagami, A. Vaishali, R. Ramakrishnan, and A. Subasini, "Weather prediction model using Savitzky-Golay and Kalman filters," *Proc. Comput. Sci.*, vol. 165, pp. 449–455, Feb. 2019.

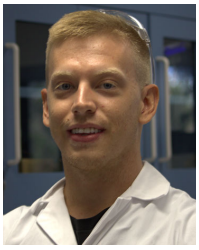
[42] M. A. Nugroho, M. Abdurohman, B. Erfianto, M. D. Sulistiyo, and A. A. Kasim, "Comparative analysis of filtering techniques in eye landmark tracking: Kalman, Savitzky-Golay, and Gaussian," in *Proc. Int. Conf. Electr., Commun. Comput. Eng. (ICECCE)*, Dec. 2023, pp. 1–6.



Waqas A. K. Afridi (Student Member, IEEE) received the B.E. degree in electronics from DUET, Karachi, Pakistan, in 2012, the M.T.M. degree from APU, Kuala Lumpur, Malaysia, in 2019, and the dual M.Res. and Ph.D. degrees from Macquarie University, Sydney, NSW, Australia, in 2021 and 2025, respectively.

With five years of industry experience, he has worked at a petrochemical plant in Saudi Arabia and an IoT firm in Pakistan. He also has over four years of casual teaching experience at Macquarie University, where he conducted Mechatronics Systems Labs and mentored Master's students on their major projects. He is currently a Postdoctoral Research Fellow with the International Center for Neuromorphic Systems, Western Sydney University, Sydney, where his work involves evaluating and integrating a range of sensor arrays for ecological health and species identification in Agri-tech environments.

Authorized licensed use limited to: Gaziantep Islam Bilim ve Teknoloji University. Downloaded on August 08,2026 at 08:18:55 UTC from IEEE Xplore. Restrictions apply.



Brady Shearan (Student Member, IEEE) received the B.Eng. (Hons.) degree in mechatronic engineering from Macquarie University, Sydney, NSW, Australia, in 2020, and the M.Res. degree from Macquarie University, North Ryde, NSW, Australia, in 2022, with a focus on impedance spectroscopy, where he is currently pursuing the Ph.D. degree in impedance metrology.

Since 2022, he has been with the National Measurement Institute Australia (NMIA), Lindfield, NSW, Australia. His research interests include impedance metrology, electrical metrology, smart sensing systems, and the Internet of Things (IoT).



Bandita Mainali is a Senior Lecturer of Civil Engineering with Macquarie University, North Ryde, NSW, Australia, with over a decade of experience in Australian universities. She has supervised more than 100 undergraduate and postgraduate students and specializes in curriculum design and accreditation compliance. Additionally, she advocates for gender diversity in engineering as the Director of Women in Engineering at MQ and is involved in various community organizations, including NEPAFE and NRNA Foundation. Her research interests include sustainable urban water management, advanced treatment technologies, and machine learning, with over 50 high-impact publications.

Dr. Mainali's teaching excellence has been recognized with multiple awards, including the PVC and VC Teaching Awards and Dean's Excellence Awards.



Subhas Chandra Mukhopadhyay (Fellow, IEEE) received the B.E.E. (Hons.) degree from Jadavpur University, Kolkata, India, in 1987, the M.E.E. degree from the Indian Institute of Science, Bangalore, India, in 1989, the Ph.D. degree from Jadavpur University, in 1994, and the D.Eng. degree from Kanazawa University, Kanazawa, Japan, in 2000.

He is working as a Professor of Mechanical/Electronics Engineering with Macquarie University, North Ryde, NSW, Australia. He has more than 35 years of teaching, industrial, and research experience. He has supervised over 40 postgraduate students and over 100 honors students. His research interests include smart sensors and sensing technology, instrumentation techniques, wireless sensors and networks, and the Internet of Things (IoT).

Dr. Mukhopadhyay is a fellow of IET (U.K.) and IETE (India). He is the Chair of the IEEE IMS NSW Chapter. He was a Distinguished Lecturer of the IEEE Sensors Council from 2017 to 2022.

Authorized licensed use limited to: Gaziantep Islam Bilim ve Teknoloji University. Downloaded on August 08,2026 at 08:18:55 UTC from IEEE Xplore. Restrictions apply.